Analyst

Accepted Manuscript

ROYAL SOCIETY OF CHEMISTRY

www.rsc.org/analyst

Journal Name

COMMUNICATION

UV Photodissociation of trapped ions following ion mobility separation in a Q-ToF mass spectrometer †

Bruno Bellina,[a] Jeffery. M. Brown,[b] Jakub Ujma,[a] Paul Murray,[b] Kevin Giles,[b] Mike Morris,[b] Isabelle Compagnon*[c] and Perdita. E. Barran*[a]

An ion mobility mass spectrometer has been modified to allow optical interrogation of ions with different mass-to-charge (*m/z*) ratios and/or mobilities (K). An ion trapping procedure has been developed which allows us to store ions for several seconds enabling UV photodissociation (UVPD).

Mass spectrometry (MS) is a versatile analytical tool, extensively used for biomolecule characterisation.[1] Over the last three decades, fragmentation techniques based on collisional or electron mediated activation have been developed to facilitate protein identification by dissociating peptides or proteins selected on the basis of their *m/z* ratio.[2-9] Fragmentation of biomolecules induced by photo-excitation of mass selected ions has also been developed, although there is, to date, no method commercially available for doing this with UV light.[10-13] The coupling of MS with tunable laser sources has greatly contributed to the development of gas-phase spectroscopy.[14] In addition to these "top-down" fragmentation approaches, ion mobility (IM) spectrometry is commonly used to rationalise differences in three dimensional structures of isobaric ions.[15-17]

Recently, the combination of IM separation with spectroscopic techniques has opened new avenues for optical studies of mass- and conformer-selected ions in the gas phase.[18-21] Inspiring results by Zucker *et al.* have showed the potential of this approach for characterization of isomeric molecules.[22] Such methods will add to the gamut of techniques that are able to distinguishing differences (or similarities) between solution and gas phase structures as well as discerning the intrinsic interactions of macromolecules.

In this paper we describe the first coupling of a Travelling Wave Ion Mobility Spectrometry (TWIMS) enabled Q-ToF mass spectrometer (Waters Synapt G2-S) with a UV laser.[16, 23] Photodissociation is demonstrated on trapped ions selected either by their *m/z* ratio, using a quadrupole mass filter, and/or by their mobility-dependent arrival time at the end of the TWIMS cell. The addition of IM separation to the UVPD approach provides an orthogonal dimension of separation, allowing the photodissociation of the arrival time (conformationally) selected ions to be performed.

The experimental setup is shown in Fig. 1. The instrument has been modified to enable overlap of the laser and the ion beam within the transfer cell region. A CaF$_2$ window is installed on the upper vacuum flange of the time-of-flight (ToF) analyser and a custom size UV-enhanced aluminium coated reflecting mirror (Melles Griot, USA) is attached to a modified pusher assembly. This mirror is mounted at a 45 degree angle with respect to the ion beam direction. In this configuration the laser beam is collinear with the ion beam. A lens has been added in the optical path, creating a focal point at the entrance of the transfer cell (between the parts 6 and 7 in Fig. 1). This modification retains all the normal functionality of the Q-ToF analyser. The laser used for this study was a Continuum Minilite II set at 266 nm with a repetition rate of 10 Hz. The energies used range between 0.4 and 1 mJ per pulse. The overall transmission of the energy between the output of the laser and the entrance of the transfer cell was measured as 50%.

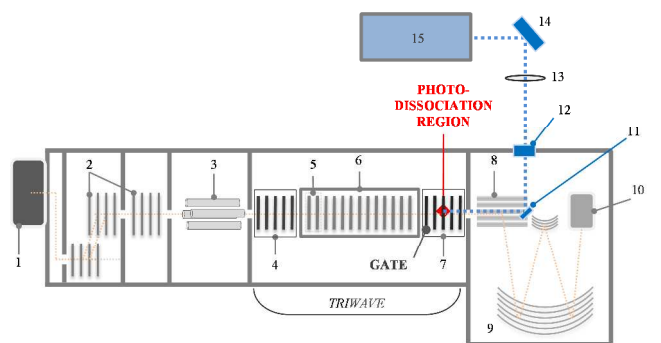**Fig. 1** Schematic of the modified Waters Synapt G2-S ion mobility enabled Q-ToF. The listed parts are: 1: Ion source; 2: Step-Wave ion guide; 3: Quadrupole; 4: Trap cell; 5: Helium cell; 6: TWIMS cell; 7: Transfer cell; 8: oa-ToF pusher assembly; 9: Dual stage reflectron; 10: Detector; 11: Fixed UV mirror; 12: Window; 13: Focusing lens; 14: Adjustable UV mirror(s); 15: Minilite 10 Hz laser 266nm.

Trapping of ions, selected by *m/z* using the quadrupole, or by arrival time using TWIMS, occurred in the transfer cell by applying a sequence of DC potentials to the exit and entrance regions. Previously it has been shown that ions can be confined for periods ranging from milliseconds to hours without significant losses.[24] During this trapping period, UV activation could be performed. The instrument control script, "WREnS" (Waters Research Enabled Software) is used to control instrument parameters and to automate the trapping process (shown in Fig.2). The trapping and gating voltages were applied using the embedded power supply of the commercial instrument.

The sequence consists of four steps: **1) Beam check**; the potentials are set to standard transmission mode (to monitor the ion beam intensity). **2) Gating & Filling**; *(2i) Gate is open* - A 3 V stopping potential is applied to the exit of the transfer cell and ions are allowed to accumulate. *(2ii) Gate closes* - A 50 V bias is applied to both TWIMS cell and gating region. Ions are defocused by the grounded exit plate of the IMS cell. Thus, only the ions matching the arrival time defined by the time dependant gate are allowed to accumulate in the transfer cell trapping region. The travelling wave (T-wave) amplitude in the transfer cell is set to a value lower than the stopping potential to prevent the ions being pushed over the exit barrier and to limit the kinetic energy applied to the trapped ions. **3) Trapping & Activation**; ions are confined and activated by the laser. During this step, the incoming ion beam is switched off by grounding the electrospray voltage and applying other stopping potentials up stream of the transfer cell (*not shown*). This ensures that the ions being confined, activated and ultimately detected are not "diluted" by unactivated ions leaking into the transfer cell. **4) Extraction**; the potentials applied at the exit of the transfer cell are decreased to axially eject the trapped ions towards the ToF analyser.
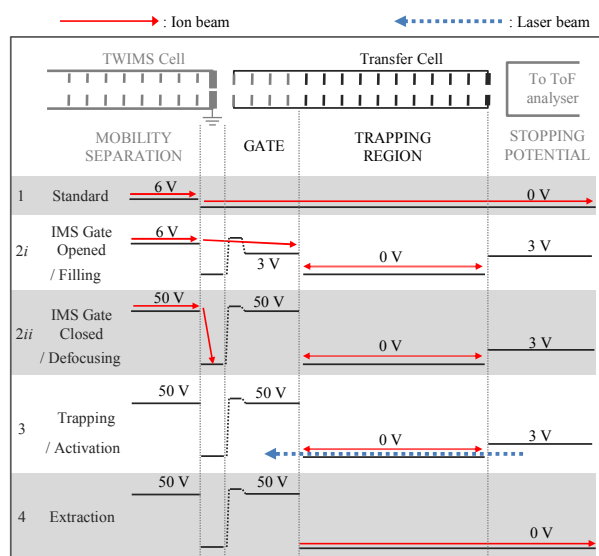

Fig. 2 Schematic of the sequences of DC potentials applied for IMS selection and trapping. *1 - Standard*; *2i & 2ii - Gating & Filling*; *3 - Trapping & Activation*; *4 - Extraction*.

Typical times used for these photodissociation experiments were: 1 second filling; and 1 second trapping. During these periods, the laser was firing and ions experience between 10 and 20 laser shots. Without trapping, ions typically pass through the transfer cell in approximately 0.5 ms. The probability of these ions being exposed to a single laser pulse is approximately 0.05%. As such, for these preliminary experiments, it was unnecessary to synchronise the laser

with the trapping step, and here the laser was allowed to fire continuously at 10 Hz. A comparison between 'trapped' and 'not trapped' UVPD mass spectra is given in the supplementary information (SUP. 1) and shows that no fragmentation occurs in the absence of trapping. The data were analysed using MassLynx Software.

The additional functionality of the instrument was evaluated using Flavin mononucleotide (FMN). (Scheme 1) In solution, this molecule absorbs in the UV and in the visible range with maximum absorption peaks at 270, 350 and 450 nm.[25] FMN was purchased as a sodium salt hydrate with a purity of 70% from Sigma Aldrich, UK. FMN solid was dissolved in a mixture of 49.5/49.5/1 methanol/water/acetic acid. This solution was infused into the instrument with the NanoLockSpray ionization source at a concentration of 10 μM. The tuning parameters for injecting the ions into the ToF analyser were set to produce a mass resolving power of 20000, for all experiments.
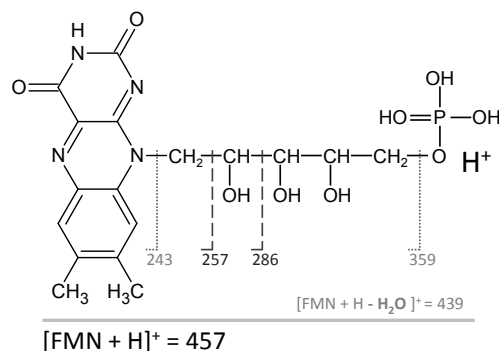

Scheme 1 Protonated Flavin mononucleotide, [FMN+H][+]. The main CID fragments (*439, 359 and 243 m/z*) (dotted line) and the two UV specific photo-fragments (*257 and 286 m/z*) (dashed line) are shown.

Initially, the TWIMS separation was disabled. The quadrupole was used to select the ion of interest and verify the UVPD of *m/z* selected ions. Fig. 3(a) shows the fragmentation spectrum of the protonated FMN, [FMN+H][+], obtained by collision induced dissociation (CID) in the transfer cell without trapping. The spectrum remains unchanged when the collisional activation occurs in the trap cell (see Fig. 1) (shown in SUP. 2). We also observe three main fragments at 439 *m/z* (loss of water), 359 *m/z* (loss of a phosphate group) and 243 *m/z* (loss of carbon side chain, lumichrome).

Fig. 3(b) shows the UVPD mass spectrum obtained. [FMN+H][+] ions were selected using the quadrupole, and accumulated for 1 second in the transfer cell. The energy of the 266 nm laser beam was estimated at 0.2 mJ per pulse in the transfer cell. There is a clear difference between the relative intensities of UVPD fragments that are in common with those generated by CID. In addition, two further product ions appear at 257 *m/z* (Lumiflavin) and 286 *m/z* (Formyl-Lumiflavin), which are typical photolysis products of flavin compounds due to electronic excitation following UV activation.[26]

UVPD spectra were also recorded of the protonated tri-peptide Tryptophan-Glycine-Tyrosine (WGY, purchased from Bachem) with a trapping time of 500 ms, and the intact Cytochrome C protein (purchased from Sigma-Aldrich) with a trapping time of 2 seconds. These compounds were prepared at a concentration of 10 μM in 50/50 water/methanol (Sigma-Aldrich) for ESI. Longer exposure times were necessary to activate larger

molecules. Classical fragmentation of the tri-peptide was observed, such as *b*-ions and loss of ammonia. (SUP. 3) A small, but consistent loss of 44 *m/z* (attributed to the carboxylic group) was found for Cytochrome C. (SUP. 4)
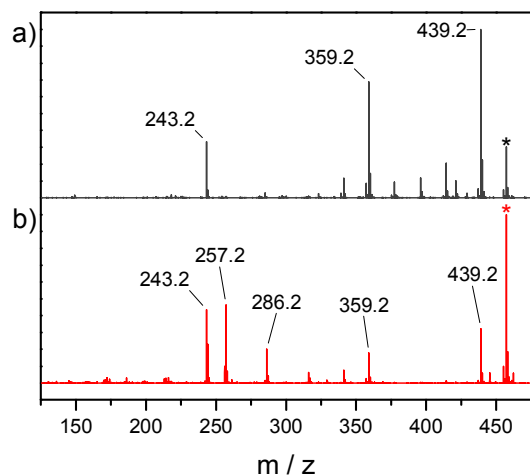
Fig. 3 The ion [FMN+H]+ (marked with a star) was first m/z selected with the quadrupole and then fragmented in the transfer cell using (a) collision induced dissociation, CID and (b) trapping and 266 nm UVPD.

UVPD spectra of ions selected by their IM separation were obtained as follows: First, the arrival time distribution (ATD) of the entire mass range was acquired. Fig. 4(a) shows the ATD of the FMN mass spectrum (black line). TWIMS parameters were adjusted to improve separation in the range of 50-600 m/z. Fig. 4(b) shows the full mass spectrum recorded with the optimized TWIMS settings. The gate parameters are defined using the 200 mobility channels (MC) of the TWIMS cell. The gate rise and fall time ranging from 1 to 1.5 MC allowed the gate width to be set, typically, to 10 MC. MassLynx software was used to extract the ATD of the [FMN+H]$^+$ ions (Fig. 4(a) - red dashed curve). Based on this, the gate was applied between the mobility channels 145 to 155 to allow ions with arrival times between 5 and 6 ms to enter the transfer cell. The ions intensity measured with and without the gate was similar, as long as the gate is larger than the distribution of the parent ions.

Once the timing of the TWIMS exit gate was set, the trapping cycle was enabled and only the arrival-time selected ions were accumulated in the transfer cell. Typically, for 1 sec filling, a hundred of cycles are completed. Fig. 4(c) shows the mass spectrum obtained when the TWIMS gate was applied. We observe a dominant species at 457 m/z, corresponding to [FMN+H]$^+$. Small peaks located both below and above 457 m/z are distinguishable. The most intense of these was at 439 m/z and corresponds to the loss of water. The presence of this ion is likely to be due to a combination of mobility overlap with [FMN+H]$^+$ as well as collisional activation during gating and the trapping steps. To reduce this collisional activation the travelling wave height and the DC potentials were set to a minimum. Fig. 4(d) shows the UVPD mass spectrum for arrival-time selected ions, trapped in the transfer cell for 1 second and irradiated with the laser. This resulted in photo-fragments with significant intensities being generated with *m/z* values of 439, 359, 286, 257 and 243. As expected these fragments are the same as those observed when the [FMN+H]$^+$ ion was selected using the quadrupole mass filter (Fig. 3(b)).

The presence of the two fragments 257 and 286 *m/z*, confirms that the fragmentation was the result of electronic excitation. We also note that the overall fragmentation was reduced by a factor of 2 when selecting by ion mobility compared with selecting by *m/z*, for the same trapping sequence. (Fig. 4(d) cf. Fig. 3(b)) This may be due to the presence of a T-wave in the transfer cell, required when the TWIMS gate is enabled. The travelling waves cause trapped ions to be driven towards the exit of the transfer cell and also increase their radial distribution. Consequently, the degree of superposition between the laser and the ion cloud may have been reduced compared to when the quadrupole was used to select the ions, and no travelling-wave was applied in the transfer cell. Future work will attempt to offset this effect by adjusting the laser focus as well as further refinement of travelling-wave parameters.
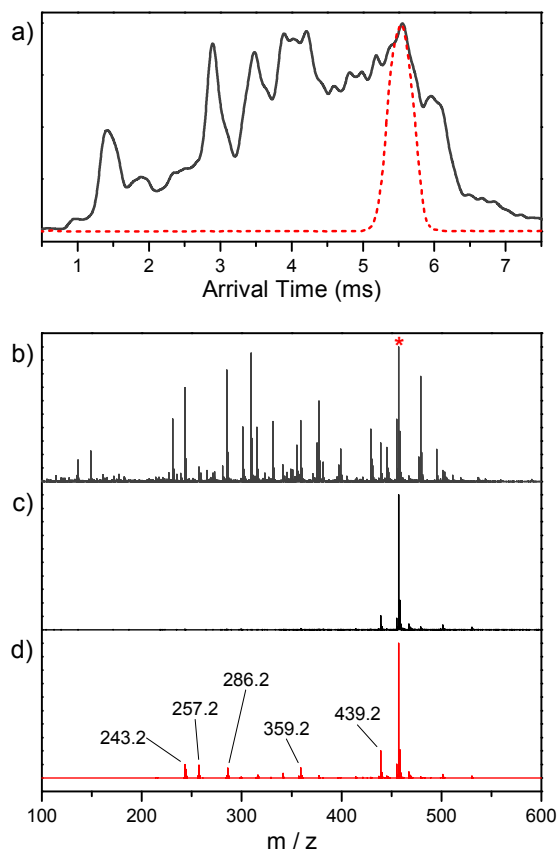

Fig. 4 (a) The black curve shows the arrival time distribution profile of the FNM mass spectrum. The red dashed curve shows the arrival time distribution profile for [FMN+H]$^+$ ion extracted from the whole spectrum. (b) FNM mass spectrum The [FMN+H]$^+$ ion is marked with a red star.(c) Mass spectrum of the TWIMS selected and trapped [FMN+H]$^+$ ion when the laser was turned off (d) Photodissociation of the arrival time selected [FMN+H]$^+$ in the transfer cell. A small amount of ions with higher *m/z* ratios were observed in the mass spectrum as they were not completely eliminated by the post TWIMS gate. Their mobility was too close to that of [FMN+H]$^+$.

Conclusions

We report the first photodissociation mass spectra recorded using ion mobility selected ions on a Q-ToF instrument. The software and hardware of the instrument have been modified to allow gating and confinement of ions following mobility separation. Introduction of the laser beam into the travelling wave assembly enabled the

protonated Flavin Mononucleotide ion to be photo-dissociated after selection by m/z (using the quadrupole mass filter) and by mobility (using the TWIMS cell). The results presented indicate that this instrument can be used for conformation-dependent photo-fragmentation and spectroscopy experiments, with great promise for future work.

Notes and references

[a] Michael Barber Centre for Collaborative Mass Spectrometry, Manchester Institute for Biotechnology University of Manchester, United Kingdom.

[b] Waters, Wilmslow, United Kingdom.

[c] Université de Lyon, Université Lyon 1, Villeurbanne, France. Institut Lumière Matière, UMR5306 Université Lyon 1-CNRS. Institut Universitaire de France IUF, 103 Blvd St Michel, 75005 Paris, France

† Electronic Supplementary Information (ESI) available: [Comparison between trapped and non-trapped UVPD spectra; comparison between CID of [FMN+H]$^+$ in the trap cell and in the transfer cell; 266 UVPD spectrum of the tri-peptide WGY; 266 UVPD spectrum of the 8$^+$ charged state Cytochrome C].
See DOI: 10.1039/c000000x/

1. R. Aebersold and M. Mann, *Nature*, 2003, **422**, 198-207.
2. B. Bogdanov and R. D. Smith, *Mass Spectrometry Reviews*, 2005, **24**, 168-200.
3. J. R. Yates, C. I. Ruse and A. Nakorchevsky, in *Annual Review of Biomedical Engineering*, 2009, vol. 11, pp. 49-79.
4. J. Mitchell Wells and S. A. McLuckey, in *Methods in Enzymology*, ed. A. L. Burlingame, Academic Press, 2005, vol. Volume 402, pp. 148-185.
5. R. A. Zubarev, N. L. Kelleher and F. W. McLafferty, *Journal of the American Chemical Society*, 1998, **120**, 3265-3266.
6. J. E. P. Syka, J. J. Coon, M. J. Schroeder, J. Shabanowitz and D. F. Hunt, *Proceedings of the National Academy of Sciences of the United States of America*, 2004, **101**, 9528-9533.
7. K. O. Zhurov, L. Fornelli, M. D. Wodrich, U. A. Laskay and Y. O. Tsybin, *Chemical Society reviews*, 2013, **42**, 5014-5030.
8. M. S. Kim and A. Pandey, *Proteomics*, 2012, **12**, 530-542.
9. R. A. Zubarev, D. M. Horn, E. K. Fridriksson, N. L. Kelleher, N. A. Kruger, M. A. Lewis, B. K. Carpenter and F. W. McLafferty, *Analytical chemistry*, 2000, **72**, 563-573.
10. V. Larraillet, A. Vorobyev, C. Brunet, J. Lemoine, Y. O. Tsybin, R. Antoine and P. Dugourd, *J Am Soc Mass Spectrom*, 2010, **21**, 670-680.
11. J. Laskin and J. H. Futrell, *Mass Spectrometry Reviews*, 2005, **24**, 135-167.
12. J. S. Brodbelt and J. J. Wilson, *Mass Spectrom Rev*, 2009, **28**, 390-424.
13. J. P. Reilly, *Mass Spectrometry Reviews*, 2009, **28**, 425-447.
14. N. C. Polfer, *Chemical Society reviews*, 2011, **40**, 2211-2221.
15. D. E. Clemmer and M. F. Jarrold, *Journal of Mass Spectrometry*, 1997, **32**, 577-592.
16. S. D. Pringle, K. Giles, J. L. Wildgoose, J. P. Williams, S. E. Slade, K. Thalassinos, R. H. Bateman, M. T. Bowers and J. H. Scrivens, *International Journal of Mass Spectrometry*, 2007, **261**, 1-12.
17. E. Jurneczko and P. E. Barran, *The Analyst*, 2011, **136**, 20-28.
18. V. Frankevich, P. Martinez-Lozano Sinues, K. Barylyuk and R. Zenobi, *Analytical chemistry*, 2013, **85**, 39-43.
19. M. Vonderach, O. T. Ehrler, P. Weis and M. M. Kappes, *Analytical chemistry*, 2011, **83**, 1108-1115.
20. B. D. Adamson, N. J. Coughlan, R. E. Continetti and E. J. Bieske, *Physical chemistry chemical physics : PCCP*, 2013, **15**, 9540-9548.
21. G. Papadopoulos, A. Svendsen, O. V. Boyarkin and T. R. Rizzo, *J. Am. Soc. Mass Spectrom.*, 2012, **23**, 1173-1181.
22. S. M. Zucker, S. Lee, N. Webber, S. J. Valentine, J. P. Reilly and D. E. Clemmer, *J Am Soc Mass Spectrom*, 2011, **22**, 1477-1485.
23. K. Giles, S. D. Pringle, K. R. Worthington, D. Little, J. L. Wildgoose and R. H. Bateman, *Rapid Commun. Mass Spectrom.*, 2004, **18**, 2401-2414.
24. J. Brown, *Poster ASMS Conference 2013*, 2013.
25. P. Drössler, W. Holzer, A. Penzkofer and P. Hegemann, *Chemical Physics*, 2002, **282**, 429-439.
26. L. Guyon, T. Tabarin, B. Thuillier, R. Antoine, M. Broyer, V. Boutou, J. P. Wolf and P. Dugourd, *J. Chem. Phys.*, 2008, **128**.